

Visible upconversion emission of Er^{3+} -doped and $\text{Er}^{3+}/\text{Yb}^{3+}$ -codoped LiInO_2^*

Research Article

Ljubica R. Djačanin^{1†}, Miroslav D. Dramićanin², Svetlana R. Lukić-Petrović¹, Dragoslav M. Petrović¹, Marko G. Nikolić²

¹ University of Novi Sad, Faculty of Sciences, Department of Physics,
Trg Dositeja Obradovića 4, 21000 Novi Sad, Serbia

² Vinca Institute of Nuclear Sciences, University of Belgrade,
P.O. Box 522, 11001 Belgrade, Serbia

Received 5 October 2011; accepted 20 January 2012

Abstract:

Lithium-indium oxide is a high-density ($5.9 \text{ g}\cdot\text{cm}^{-3}$), wide band-gap semiconductor with promising applications for scintillating detection of solar neutrinos as well as for efficient phosphorescence when doped with Er^{3+} or Sm^{3+} ions. In this report, we demonstrate visible upconversion emission of Er^{3+} -doped LiInO_2 synthesized by a simple solid-state chemistry procedure and discuss mechanisms responsible for pumping the Er^{3+} ions to upper levels. Intense upconversion emission is observed in the green and red spectral regions under near-infrared excitation, and it is greatly enhanced by co-doping with Yb^{3+} ions. We also examined the upconversion intensity change as a function of temperature, and, consequently, possible applications of this material as a low-temperature sensor.

PACS (2008): 78.55.Hx

Keywords: LiInO_2 • upconversion • temperature sensing • Er^{3+} • Yb^{3+}
© Versita Sp. z o.o.

1. Introduction

Double oxides of indium might comprise a new family of high-density ($\geq 6 \text{ g}\cdot\text{cm}^{-3}$) scintillators and phosphors. The distance between the cation and the surrounding oxygen ions is short, favoring a high light output. The indium background β^- (495 keV maximum) decay rate per mol is about 316 times lower than in natural lutetium con-

taining radioactive ^{176}Lu . Therefore, mixed indium oxide can be used in nuclear applications requiring a large-volume scintillator instead of lutetium-based compounds [1]. Also, it has a possible application as a scintillator for the detection of low-energy solar neutrinos due to the inverse β^- -decay of ^{115}In to ^{115}Sn [2]. Lithium-indium oxide can also be applied in energy-storage and -conversion devices [3]. When doped with rare-earth ions, LiInO_2 becomes a promising phosphor material [4]. However, there are very few reports in the literature on the photoluminescent properties of lithium-indium oxide doped with different rare-earth ions. In recent years, advances in both solid-state lasers and semiconductor laser diodes have

*presented at the 3rd International Workshop on Advanced Spectroscopy and Optical Materials, July 17–22, 2011, Gdańsk, Poland

†E-mail: ljubica@df.uns.ac.rs

resulted in more efficient IR sources. As a result, upconversion, where the absorption of two or more low-energy photons is followed by the emission of a higher-energy photon, has attracted significant attention. Trivalent rare-earth ions, such as Er³⁺, Tm³⁺, Ho³⁺, and Yb³⁺ are the ones that commonly exhibit the upconversion phenomenon. Among these, Er³⁺ is the most popular because its metastable levels, such as ⁴I_{9/2} and ⁴I_{11/2}, are easily accessible with NIR radiation and can be conveniently populated by commercial low-cost high-power laser diodes [5]. There are various processes that can lead to emission at wavelengths shorter than the excitation wavelength [6]. In general, the most efficient are energy-transfer upconversion (ET) and excited-state absorption (ESA). The sensitization of rare-earth doped materials with Yb³⁺ ions is a well-known method for increasing the upconversion intensity because of the high absorption cross-section of Yb³⁺ ions around 980 nm and the efficient energy transfer from Yb³⁺ to other rare-earth ions [7–9]. In this paper, we report an efficient infrared-to-visible upconversion for LiInO₂:Er and LiInO₂:(Er,Yb) powders synthesized by a simple solid-state preparation method. Excited-state absorption and energy-transfer processes are discussed as possible mechanisms for the upconversion emissions of the samples. In addition, we investigated the upconversion intensity change within the temperature range of 10–300 K and the possibility of using these samples as temperature sensors for low temperatures.

2. Experimental

Samples of LiInO₂:Er (3 at%) and LiInO₂:(Er,Yb) (1.5+1.5 at%), with compositions Li[In_{0.88}Er_{0.12}]O₂ and Li[In_{0.88}Er_{0.06}Yb_{0.06}]O₂, respectively, were synthesized using a simple solid-state procedure described in detail elsewhere [10]. The starting components were In₂O₃ (Aldrich, 99.99%) and Li₂CO₃ (Kemika, p.a.), and the dopant precursors were Er₂O₃ (Aldrich, 99.99%) and Yb₂O₃ (Alfa Aesar, 99.9%). Phase purity of the samples was confirmed by X-ray diffraction measurements that were performed on a Philips PW 1050 instrument using Ni filtered Cu K_{α1,2} radiation.

Diffraction data was recorded in a 2θ range from 10° to 70° counting for 10 s in 0.02° steps. Photoluminescence excitation and emission spectra and lifetime measurements were performed on a high-resolution spectrofluorometer system, which is comprised of an optical parametric oscillator excitation source (EKSPLA NT 342, emission range 210–2300 nm), a Cryostat (Advance Research Systems), a spectrograph FHR 1000 (Horiba Jobin-Yvon, 1800 groove/mm grating), and an

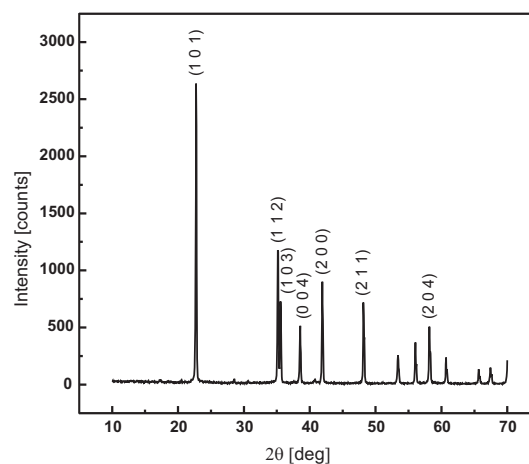


Figure 1. XRD pattern of the Er-doped sample.

ICCD detector (Horiba Jobin-Yvon).

3. Results and discussion

3.1. XRD and crystal structure

LiInO₂ crystallizes in a tetragonal α-LiFeO₂-type structure with space group *I*₄/*amd* [11]. In this structure, indium ions are octahedrally coordinated with oxygen ions where each InO₆ octahedron shares edges with other InO₆ octahedra. Since Er³⁺ (Yb³⁺) ions substitute In³⁺ in the α-LiFeO₂ structure, they are also octahedrally coordinated and occupy sites with *D*₂*d* symmetry (no inversion center). Figure 1 presents the XRD pattern of the LiInO₂:Er sample with peaks indexed according to the JCPDS 43-1131 diffraction data. Both samples are of a single-phase nature with no impurity peaks noticed.

3.2. Upconversion emission investigations

Figure 2 presents the upconverted emission spectra of the LiInO₂:Er sample obtained using a 1540 nm excitation at different temperatures ranging from 300 K down to 10 K. The spectra exhibit three emission bands in the visible range corresponding to the transitions from the excited states of the Er³⁺ ion. Bands in the green region of 516–529 nm and 532–580 nm are assigned to the transitions ²H_{11/2} → ⁴I_{15/2} and ⁴S_{3/2} → ⁴I_{15/2}, respectively, while the red-region band of 640–710 nm is associated to the ⁴F_{9/2} → ⁴I_{15/2} transition [12–14]. The influence of codoping with Yb³⁺ ions is presented in Figure 3. The room-temperature spectra of the LiInO₂:Er and LiInO₂:(Er,Yb) samples, acquired with a 980 nm excitation, show that

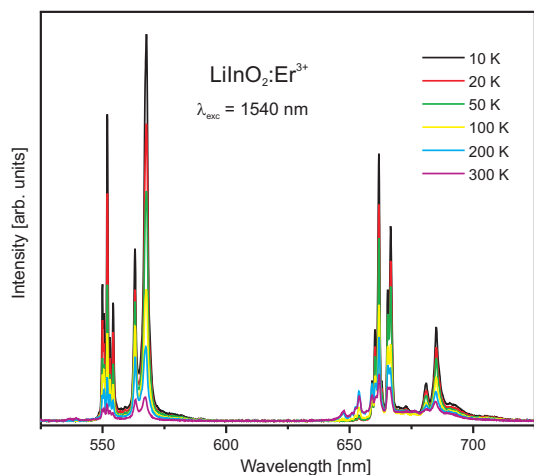


Figure 2. Upconversion emission spectra of the Er-doped sample. Excitation wavelength: 1540 nm.

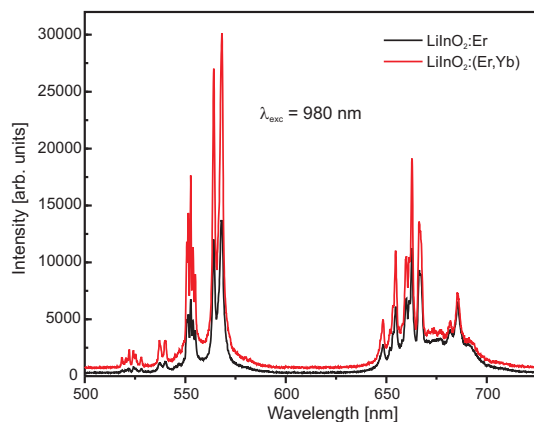


Figure 3. Upconversion emission spectra of both samples. Excitation wavelength: 980 nm.

the integrated emission intensity increases by a factor of 2.1 for green and a factor of 1.4 for red emission. The lifetimes of the samples were measured at 567 nm and 661 nm, which are the wavelengths of the most intense transition in the green and red region, respectively. The lifetime values do not vary much and are around 0.5 ms for both samples at different temperatures.

The upconversion mechanisms are shown in Figure 4 and Figure 5 for Er-doped and (Er,Yb)-doped samples, respectively. For the Er-doped sample excited with 1540 nm radiation, we assumed that a three-photon process contributes to the upconversion emission (see Figure 4). The laser excitation brings the Er^{3+} ion to the $^4I_{13/2}$ level, after which excited-state absorption (ESA) occurs twice in order to reach the first emitting $^2H_{11/2}$ level. After that, the

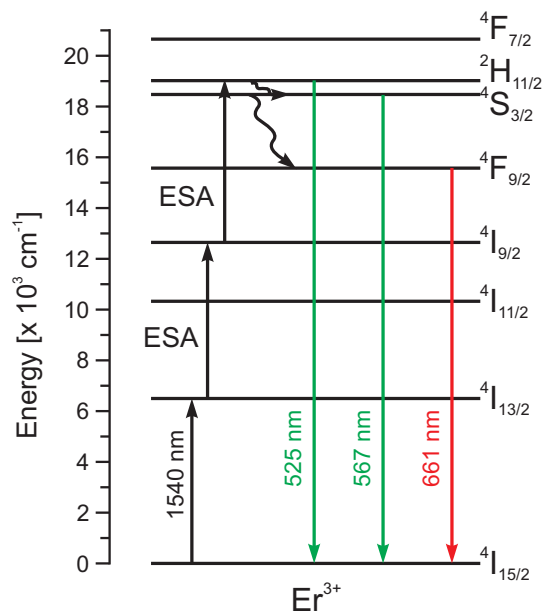


Figure 4. Possible upconversion mechanism for the Er-doped sample; excitation at 1540 nm.

Er^{3+} ion non-radiatively relaxes to the lower emitting levels ($^4S_{3/2}$ and $^4F_{9/2}$) by multiphonon decay. The upconversion mechanism of the (Er,Yb)-doped sample excited with 980 nm radiation is depicted in Figure 5. Er^{3+} ions can be excited to the $^4I_{11/2}$ level both by ground-state absorption of the Er^{3+} ion itself and by energy transfer from excited Yb^{3+} ions (ET2). The latter is the dominant mechanism [8], since the Yb^{3+} ion has a larger absorption cross-section around 980 nm than the Er^{3+} ion. Ions in the $^4I_{11/2}$ level can be further excited to the $^4F_{7/2}$ level by excited-state absorption of the Er^{3+} ion (ESA) or by energy transfer (ET1) from Yb^{3+} ions. Consequently, the emitting levels ($^2H_{11/2}$, $^4S_{3/2}$, and $^4F_{9/2}$) are reached by non-radiative relaxation. However, to obtain a better understanding of the mechanism(s) of upconversion, a power-dependence study of the luminescence intensity should be performed, and this will be the subject of further investigations.

3.3. Temperature sensing using upconversion

In order to evaluate the possibility of using Er-doped LiInO_2 phosphor as a temperature sensor for low temperatures, we examined the luminescence-intensity change for the temperature range of 10–300 K. To eliminate errors that can occur by using intensity-based techniques (the observed intensity is also a function of other variables apart from temperature) [15], we used the intensity-ratio

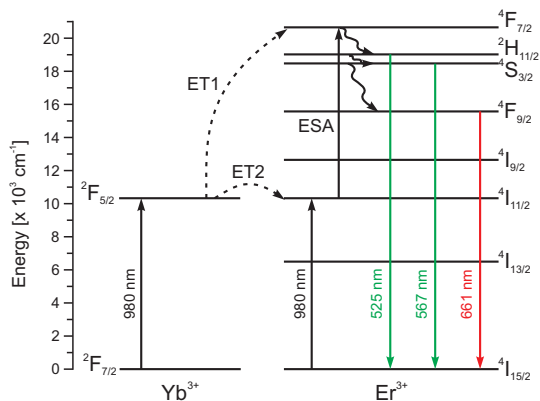


Figure 5. Possible upconversion mechanism for (Er,Yb)-codoped sample; excitation at 980 nm.

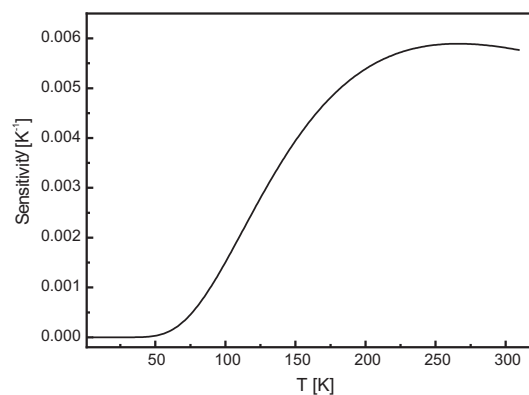


Figure 7. Temperature sensitivity of the Er-doped sample as a function of temperature.

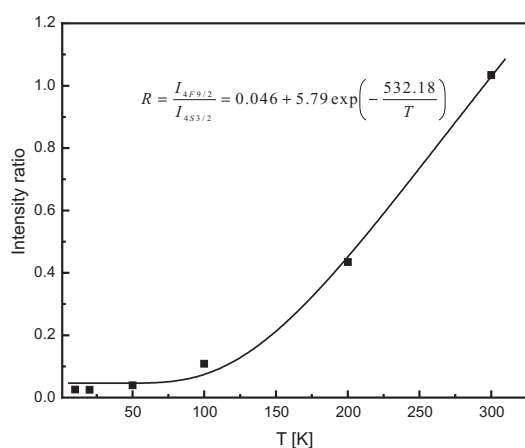


Figure 6. Intensity ratio of emissions from the ⁴S_{3/2} and ⁴F_{9/2} levels as a function of temperature.

mode. When the intensity-ratio method is employed, the ideal conditions are that the intensities of two emission lines show different responses to temperature [15], and that the emission intensity is strong enough to avoid optical noise [16]. We investigated the intensity ratio of the emissions from the ⁴S_{3/2} and ⁴F_{9/2} levels excited by 1540 nm radiation (see Figure 2). We found that the intensity ratio of these emission lines depends strongly on the temperature, and the dependence is fitted with an exponential function. This is shown in Figure 6. The temperature sensitivity, $S = \left| \frac{dR}{dT} \right|$, is obtained as the first derivative of the measured fluorescence-intensity ratio. Figure 7 shows that the sample LiInO₂:Er³⁺ exhibits significant temperature sensitivity for the temperature range of 50–300 K, being most sensitive (about 0.0055 K⁻¹) in the 175–300 K region.

4. Conclusions

LiInO₂:Er³⁺ and LiInO₂:(Er,Yb) phosphor powders were successfully obtained using a simple and fast solid-state synthesis method. Both samples exhibit intense upconversion emission in the visible range after near infra-red excitation, which is typical for Er³⁺ ions. The emission intensity is greatly enhanced by co-doping with Yb³⁺ ions. The emission lifetimes of the samples are around 0.5 ms. The sample LiInO₂:Er³⁺ exhibits significant temperature sensitivity for the temperature range of 50–300 K, which makes this material a good candidate for temperature sensing of low temperatures.

Acknowledgements

The authors acknowledge financial support from the Ministry of Science and Education of the Republic of Serbia (project No. OI 171022) and from the Provincial Secretariat for Science and Technological Development of the Government of Vojvodina (project No. 114-451-2187).

References

- [1] M. Balcerzyk et al., IEEE Nucl. Sci. Symp, IEEE Trans. Sci. 6, 25 (2000)
- [2] K. Kushida, T. Koba, K. Kuriyama, J. Appl. Phys. 93, 2691 (2003)
- [3] G-Q. Zhang, S-T. Zhang, X-F. Wu, Phys. Stat. Sol. A 207, 101 (2010)
- [4] S.A. Naidu, U.V. Varadaraju, Electrochem. Solid-State Lett. 11, J44 (2008)
- [5] H. Lin et al., J. Appl. Phys. 93, 186 (2003)

- [6] F. Auzel, *Chem. Rev.* 104, 139 (2004)
- [7] F. Vetrone, J.C. Boyer, J.A. Capobianco, A. Speghini, M. Bettinelli, *J. Phys. Chem. B* 107, 1107 (2003)
- [8] S. Xu *et al.*, *Chem. Phys. Lett.* 385, 263 (2004)
- [9] A.S. Oliveira *et al.*, *Appl. Phys. Lett.* 72, 753 (1998)
- [10] Lj.R. Djačanin *et al.*, *Phys. Status Solidi C* 8, 2830 (2011)
- [11] H. Glaum, S. Voigt, R. Hoppe, *Z. Anorg. Allg. Chem.* 598, 129 (1991)
- [12] G.S. Maciel, M.A.R.C. Alencar, C.B. de Araujo, A. Patria, *J. Nanosci. Nanotechnol.* 10, 2143 (2010)
- [13] H. Guo, *et al.*, *J. All. Comp.* 415, 280 (2006)
- [14] A.S.S. de Camargo, *et al.*, *J. Phys. Condens. Matter* 19, 246209 (2007)
- [15] A.H. Khalid, K. Kontis, *Sens.* 8, 5673 (2008)
- [16] N. Ishiwada, S. Fujioka, T. Ueda, T. Yokomori, *Opt. Lett.* 36, 760 (2011)